Heliyon 9 (2023) e23284

Contents lists available at ScienceDirect

Heliyon

journal homepage: www.cell.com/heliyon

Polyimide biocomposites coated with tantalum pentoxide for stimulation of cell compatibility and enhancement of biointegration for orthopedic implant

Syed Asadullah [a,*], Mahmood Ahmed [b,**], Sadaf Sarfraz [c], Manzar Zahra [c], Asnuzilawati Asari [d,***], Nurul Huda Abdul Wahab [d], Farah Sobia [e], Dure Najaf Iqbal [f]

[a] Chandbagh College Kot Jilani, Muridke-Sheikhupura Road, Muridke, Pakistan
[b] Department of Chemistry, Division of Science and Technology, University of Education, Lahore-54770, Pakistan
[c] Department of Chemistry, Lahore Garrison University, Lahore, Pakistan
[d] Faculty of Science and Marine Environment, Universiti Malaysia Terengganu, 21030 Kuala Nerus, Terengganu, Malaysia
[e] Punjab Food Authority, 83-C, Muslim Town, Lahore-Pakistan
[f] Department of Chemistry, The University of Lahore, Lahore-Pakistan

ARTICLE INFO

Keywords:
Biocomposites
Bone implant
BMSCs
Biocompatibility
Bioactivity
Osteoclast

ABSTRACT

Orthopedic implants are an important tool in the treatment of musculoskeletal conditions and helped many patients to improve their quality of life. Various inorganic-organic biocomposites have been broadly investigated particularly in the area of load-bearing orthopedic/dental applications. Polyimide (PI) is a promising organic material and shows excellent mechanical properties, biocompatibility, bio-stability, and its elastic modulus is similar to human bone but it lacks bioactivity, which is very important for cell adhesion and ultimately for bone regeneration. In this research, tantalum pentoxide (Ta_2O_5) coating was prepared on the surface of PI by polydopamine (PDA) bonding. The results showed that Ta_2O_5 was evenly coated on the surface of PI, and with the concentration of Ta_2O_5 in the PDA suspension increased, the content of Ta_2O_5 particles on the surface of PI increased significantly. In addition, the Ta_2O_5 coating significantly increased the roughness and hydrophilicity of the PI matrix. Cell experiments showed that PI surface coating Ta_2O_5 could promote the proliferation, adhesion, and osteogenic differentiation of bone marrow-derived stromal cells (BMSCs). The results demonstrated that fabricating Ta_2O_5 coating on the surface of PI through PDA bonding could improve the biocompatibility as well as bioactivity of PI, and increase the application potential of PI in the field of bone repair materials.

1. Introduction

With the population aging, the incidence of orthopedic and dental defects caused by trauma, tumor resection, or congenital deformity is increasing rapidly so governments all over the world have to increase budgets to maintain the increasing expenses for

* Corresponding author.
** Corresponding author.
*** Corresponding author.
E-mail addresses: syedasadullah7@gmail.com (S. Asadullah), mahmoodresearchscholar@gmail.com, mahmood.ahmed@ue.edu.pk (M. Ahmed), asnu@umt.edu.my (A. Asari).

https://doi.org/10.1016/j.heliyon.2023.e23284
Received 17 July 2023; Received in revised form 26 October 2023; Accepted 30 November 2023
Available online 3 December 2023

healthcare every year [1,2]. Now, the most common orthopedic/dental materials are metals such as titanium (Ti) alloys because of their outstanding corrosion resistance, better mechanical strength, good biocompatibility, and osseointegration properties [3–5]. However, there are concerns regarding the probable release of harmful metal ions and radiopacity among metal alloys and natural bones [6]. Also, the mismatch of elastic modules between metal alloys and cortical bone of a human being results in bone decline [7]. Some serious difficulties after surgery such as allergenicity, loss and unsatisfactory integration among the implant and bone as well as eventual implant failure might occur. To overcome these limits and reduce negative biological reactions after implantation, alternatives of metals are broadly followed [8–10].

Over the past decades, inorganic-organic biocomposites in the biomedical field have been broadly investigated particularly in the area of load-bearing orthopedic/dental applications [11–13]. Organic materials e.g. synthetic polymers have excellent mechanical properties, thermal stability, and environmental resistance, but inorganic materials such as metal oxide, and bioceramics/glasses attribute almost no cytotoxicity and appreciable bioactivity [14,15]. One of the potential organic materials is polyimide (PI), which is an amorphous and non-degradable polymer that shows several prominent properties biomedical field for orthopedic/dental applications. For instance, exhibits outstanding biocompatibility, bio-stability, excellent mechanical behaviors, and elastic modulus comparable to human bone [16–19]. The non-toxic effect of PI has been verified specifically in vitro and in vivo results, which might have shown slightly less hemolysis and it is anticipated that PI can become a new inorganic biomaterial in the field of orthopedic/dental applications. In spite, PI exhibits outstanding biocompatibility, it is bioinert material but shows weak bioactivity that is very important for cell adhesion and ultimately for bone regeneration. So, how to enhance the bioactivity as well as stimulating the integration of bone implants of PI will become a great challenge in orthopedic and dental applications [20–22].

Surface modification is considered as a productive technique to enhance the surface mechanical and biological properties although the favorable to the whole properties of the biomaterials might be sustained [23]. To enhance the bioactivity of biomaterials and facilitate their surface for orthopedic/dental applications, several different techniques have been utilized to modify and functionalize the biomaterial's surface [24]. For example, blended with bioactive materials, bioactive coatings (e.g., calcium phosphate, hydroxyapatite) grafting specific functional groups, spin-coating, electron beam deposition, and regulating surface topography, which might improve bioactivity, surface roughness, and other biological properties, etc. However, these surface modifications enhance the surface bioactivity of biomaterial but unfortunately, these approaches still have some drawbacks and limitations e.g. particular apparatus, and rigorous conditions that delay their application for orthopedic/dental implantation [25]. Therefore, to avoid such restrictions (PDA) coating or surface modification is a good alternative method to improve the surface bioactivity of biomaterial, which could have long-term stability and osteoblast response [26].

In the last few years, tantalum (Ta) metal has been known for outstanding strength and anticorrosion properties, and even it is insoluble in water and acidic medium [27,28]. It also has better biocompatibility. The Ta metal surface has a natural oxide (tantalum pentoxide), which plays an important influence on the biocompatibility of the Ta metal [29]. Tantalum pentoxide (Ta_2O_5, TO) were getting great consideration in dental and orthopedic applications without toxic effect. The better chemical and thermal stability of the TO along with their bioactivity and high biocompatibility is beneficial after implantation for long-term stability [30]. Although the most stable form of Ta metal is the pentavalent state, it was confirmed that equally capable of having several states of oxidation in unsaturated TO. Previous studies have confirmed that TO has good biocompatibility and bioactivity which might enhance cell adhesion, proliferation, and differentiation [31]. The TO is beneficial for the natural hard tissue through the materialization of the bone-like apatite layer [32]. TO may provide a good alternative to the other materials because of its good corrosion resistance and excellent biocompatibility [33]. In addition, TO showed hydrophilicity, surface roughness, and improved cell-material interactions in previous studies which confirmed that TO offered a promising surface biological environment for cell adhesion, proliferation, and differentiation [34].

This research presents the development of bioactive coating and accelerates the biological responses of the surface of PI for orthopedic and dental applications. The study's main objective is to increase the biointegration of orthopedic implants. This involves determining whether TO covering PI biocomposites (DTPC) can improve the integration of the implant with the surrounding bone and tissue. The second important goal is identifying whether coated PI biocomposites promote improved cell compatibility and examining whether TO coating encourages the effective implant integration process namely cell adhesion and proliferation. Besides, the microporous coating containing TO particles can improve the biological properties of the surface for the cellular response. Therefore, the surface properties (e.g., roughness, micromorphology, composition, and hydrophilicity) of DTPC were characterized. Furthermore, the apatite mineralization of DTPC in simulated body fluid (SBF) was estimated. In addition, the cellular response (proliferation, adhesion, and alkaline phosphatase activity) of bone mesenchymal stem cells (BMSC) of rats to DTPC were observed and studied in vitro.

2. Materials and methods

2.1. Preparation of TO coating

Tantalum pentoxide (TO) (Aladdin Co., Shanghai, China) and polyimide (PI) (Junhua Co., Jiangsu, China) powders were utilized as the elementary materials, followed both powders were cleaned by ethanol and deionized water followed by drying in an oven at 37 °C. The PDA solution (2 mg/mL) by dissolving dopamine phosphate buffer saline (PBS) with TO particles was prepared by adding TO into a prepared solution of PDA at ambient temperature. The prepared solution was put into an ultrasonic cleaner (KQ5200DE, Kun Shan Ultrasonic Instruments Co., Ltd., China) for the proper dispersion of the TO particles for 15 min. PI square parallelepiped samples (diameter of 12 inches and thickness of 2 mm) were prepared through the pressing and sintering process by using a mold. Before the

experiment, the PI samples were ground with #800 sandpaper. To remove impurities, the samples were cleaned with ethanol, acetone, and deionized water respectively before surface modification/treatment. The PI samples were immersed in PDA solution with a different concentration of TO particles (1.5 wt % and 1.5 wt %) for 6 and 12 h at ambient temperature. Furthermore, modified PI samples were labeled as PI, DTPC6, and DTC12 respectively. Lastly, the samples were taken out and then dried for 24 h at 70 °C for further use.

2.2. Characterization of TO coating

The crystalline phase of TO particles was examined by an X-ray diffractometer (XRD, CuKα radiation, Japan), the diffraction angles (2θ) were set between 10° and 80°, Fourier transform infrared spectrometry (FTIR, Nicolet 6700, Nicolet, USA). A scanning electron microscope (FE-SEM, S-4800, HITACHI, Japan) equipped with an energy dispersive spectrometer (EDS) was performed to identify both the morphology and chemical constituent of PI, DTPC6, and DTPC12 samples. As well, the roughness of the samples was detected using a 3-D laser confocal microscope (LCM, VK-X 110, Keyence Co., Japan). To measure the hydrophilic properties of samples water contact angles were measured with the sessile droplet method in a contact angle measuring device (CAM, JC2000C1, Powereach Co., China).

2.3. In vitro apatite mineralization

SBF solution was utilized to assess the mineralization of the PI, DTPC6, and DTPC12 samples, and SBF solution was prepared by the predefined method in the previous study [16]. The chemical compositions of both SBF and human plasma are almost equivalent [35, 36]. The samples were soaked for 1, 3, 7, 10, and 14 days in SBF at 37 °C, and samples were carefully taken out, very gently cleaned with distilled water, and dried overnight. The surface microstructures and composition of immersed samples were examined through FE-SEM equipped by EDS.

2.4. In vitro cytocompatibility

2.4.1. Cell culture

BMSCs, which are bone marrow-derived stromal cells were utilized in this research (Cell Bank, Chinese Academy of Science (Shanghai, China)). BMSCs cells were cultured α-minimum essential medium (α-MEM, Thermo Fisher Scientific Inc., USA) having 10 % fetal bovine serum (FBS) and placed at 37 °C in the atmosphere of 5% CO_2. The medium of cell culture was substituted every 3 days interval. All groups of samples (PI, DTPC6, and DTPC12) were placed in 24-well plates, which were cleaned with 75 % ethanol for 1 h and washed with sterile phosphate-buffered saline (PBS) thrice before cell culturing. The BMSCs were seeded onto the samples with a density of 2×10^4 cells/well, which was used for cell adhesion, proliferation, and osteogenic differentiation.

2.4.2. Cell adhesion

The BMSCs were seeded in each well with a density of 2×10^4, co-cultured for 1 day, and measured by SEM and confocal laser scanning microscopy (CLSM) to detect the spreading of cells. SEM was used to see the cytoskeleton. The PBS was used to carefully wash the samples thrice and samples were soaked in 2.5 % glutaraldehyde solution overnight to fix the cells in the samples at room temperature. Subsequently, the cells were dehydrated in graded ethanol (10, 30, 50, 70, 90, and 100 %; 15 min each) and samples were dried at 37 °C and gold sputtering, all the samples were observed using SEM. The cytoskeleton protein F-actin was stained by fluorescein isothiocyanate (FITC; Sigma) for half an hour and 4′, 6′-diamidino-2-phenylindole (DAPI; Sigma) for 8 min. Finally, the stained cells (fluorescence images) on samples were detected with confocal laser scanning microscopy (CLSM; Nikon A1R, Nikon Co. Ltd., Japan).

2.4.3. Cell proliferation

The proliferation cell at 1, 3, and 7 days was determined by culturing cells with a density of 2×10^4 cells per sample and the medium was changed every 3 days. The growth of the cell, specified with the optical density (O.D.), was evaluated with a methylthiazol tetrazolium test (MTT). The culture medium was changed with Minimum Essential Medium Eagle - Alpha Modification (α-MEM, 400 μL) and MTT solution (100 μL, Amresco Co., USA) after the cultivation for 4 h. Afterward, the medium was changed by 500 μL dimethyl sulfoxide (DMSO, Sinopharm Co., Shanghai, China) for half an hour. The O.D. value was observed at 490 nm by a microplate reader.

2.4.4. Alkaline phosphatase activity

The osteogenic activity of BMSCs was measured by examining the alkaline phosphatase (ALP) activity of the BMSCs on the samples, the protocol cell culturing was quite similar to that mentioned earlier. At specific times (7, 10, and 14 days) cultured on the samples, the culture media was taken out, and the samples were washed thrice by PBS. In addition, the lysate was made by adding 200 mL of 1 % Nonidet P-40 (NP-40) for 60 min. Afterward, 50 mL of the supernatant was placed in the 96-well plates, which was pursued with the addition of r-nitrophenyl phosphate (Sigma, Singapore) solution of a substrate 0.1 mol L^{-1} glycine and 1 mol L^{-1} $MgCl_2 \cdot 6H_2O$. Finally, later incubating at 37 °C for 60 min, the reaction was seized by the addition of 100 m/L solution of 2 M NaOH. The absorbance of ALP was assessed at 450 nm through a microplate reader. The concentration of whole protein was determined in cell lysate by a bicinchoninic Acid (BCA) process into aliquots of similar samples via the Pierce protein analysis kit (Pierce Biotechnology Inc., USA) at a wavelength of 450 nm and measured concerning an order of albumin (bovine serum albumin) environments.

2.5. Statistical analysis

All data were derived from independent experiments using BMSCs, the results were measured independently and each parameter was investigated in triplicate. The data was indicated as the mean ± standard deviation (M ± SD) and the results of the in vitro experiments were statistically analyzed by the one-way ANOVA. The obtained result is significant statistically, by the standards of the study, if $p < 0.05$.

3. Results

3.1. Characterization of PI and DTPC samples

3.1.1. FTIR spectral analysis

Fig. 1a shows the FTIR spectra of the PI, DTPC6, and DTPC12 samples. The absorption peaks for PI were detected at nearly 1780 cm^{-1} (asymmetrical stretching of C═O), 1724 cm^{-1} (symmetrical stretching of C═O), and 1380 cm^{-1} (stretching of C–N), and 725 cm^{-1} (bending of C═O). The absorption peaks for TO were detected at nearly 880 cm^{-1} (bridge of Ta–*O*–Ta) and 680 cm^{-1} (stretching of Ta–O). So the FTIR spectroscopy confirmed the successful coating of TO.

The XRD patterns of PI, DTPC6, and DTPC12 samples are shown in Fig. 1b. The wide peak at $2\theta = 17.5°–30°$ specified the amorphous phase of PI. As well, the peaks of $2\theta = 22.8°$, 28.4°, 36.7°, 46.8°, 50.4°, and 55.6° could be detected, which were the characteristic peaks of TO. All the characteristic peaks of PI and TO were detected in the DTPC6 and DTPC12 samples.

3.1.2. Surface morphology and elemental distribution

The surface morphologies of PI, DTPC6, and DTPC12 samples have been illustrated by SEM as shown in Fig. 2a–f. In addition to this, the surfaces of PI samples in Fig. 2a–d have clearly displayed smooth topography with few cracks. In Fig. 2b–f, it has been observed that TO particles appear homogeneously distributed after the coating of TO, and these TO particles are well interconnected with the PI surface (DTPC surfaces). DTPC12 in Fig. 2c–f displayed a rough surface as compared to DTPC6 in Fig. 2b–e.

Fig. 3a, d, and 3g show the spectrum of EDS PI, DTPC6, and DTPC12 samples. The peaks of C and O elements were observed in the samples of PI, but meanwhile, O and Ta elements were observed in DTPC6 and DTPC12. In the EDS distribution maps, it was detected C, O, and Ta elements displayed uniform distribution in the composites. Fig. 3b, e, and 3h represent the elemental mapping of C, O, and Ta for DTPC6 whereas the elemental mapping of C, O, and Ta for DTPC12 is presented by 3c, 3f, and 3i respectively.

3.1.3. Surface roughness

The laser confocal microscope 3D images of PI, DTPC6, and DTPC12 are shown in Fig. 4a–c. The roughness of the samples has been demonstrated in Fig. 4d. The roughness (Ra) of the PI, DTPC6, and DTPC12 samples was 2.263 μm, 4.596 μm, and 6.512 μm.

3.1.4. Water contact angles and protein adsorption

Fig. 5a displays the water contact angles of PI, DTPC6, and DTPC12 samples. The addition of to the PI influenced the hydrophilicity, defined through water contact angles. The water contact angles reduced from 81° on PI to 58.5° and 36.5° on DTPC6 and DTPC12 respectively. The illustrative images of droplets of water also revealed consistent results, significance that the TO efficiently enhanced the hydrophilicity.

Fig. 5b represents the protein adsorption on the PI, DTPC6, and DTPC12 samples. The amount of protein adsorption on the PI, DTPC6, and DTPC12 samples was 5.8 ± 0.25, 15 ± 0.31, and 23 ± 0.50 mg/g respectively. Significantly more protein is adsorbed on the DTPC surfaces with the increase of TO content than that absorbed on the PI surface.

3.2. Apatite mineralization

The SEM images in Fig. 6 a-c display the surface morphology of the samples (PI, DTPC6, and DTPC12) after immersing in SBF for 7

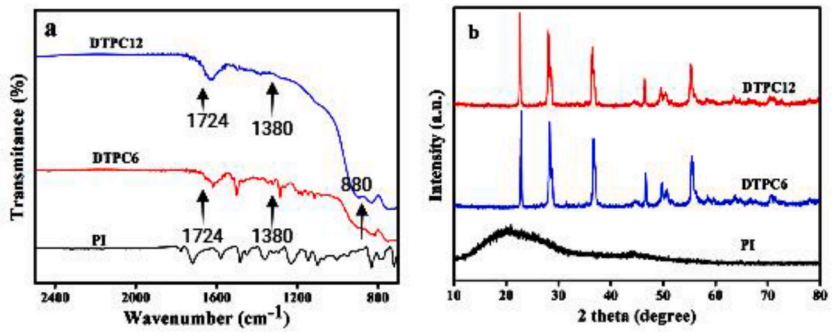

Fig. 1. Ftir (a), XRD (b) of PI, DTPC6 and DTPC12.

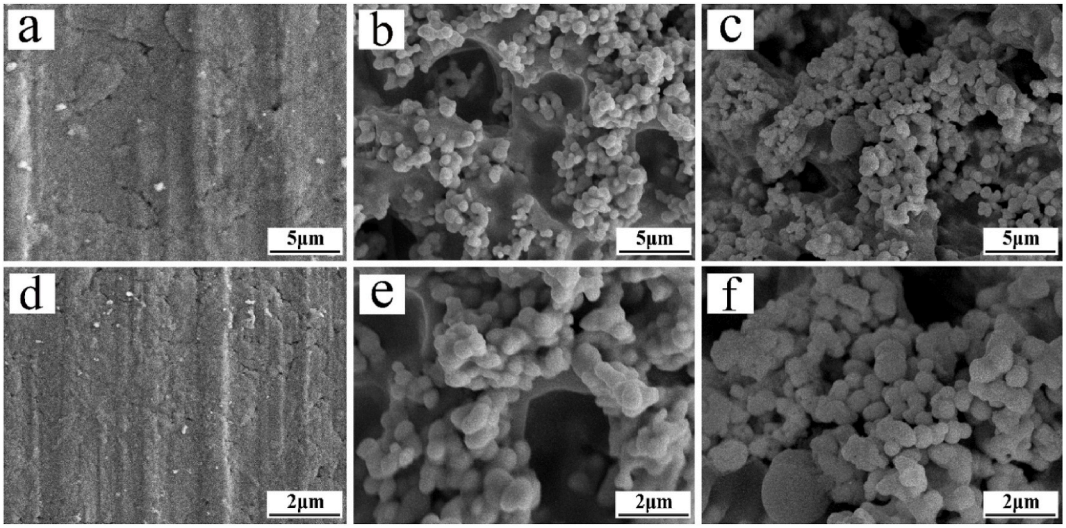

Fig. 2. SEM images PI (a, d), DTPC6 (b, e), and DTPC12 (c, f).

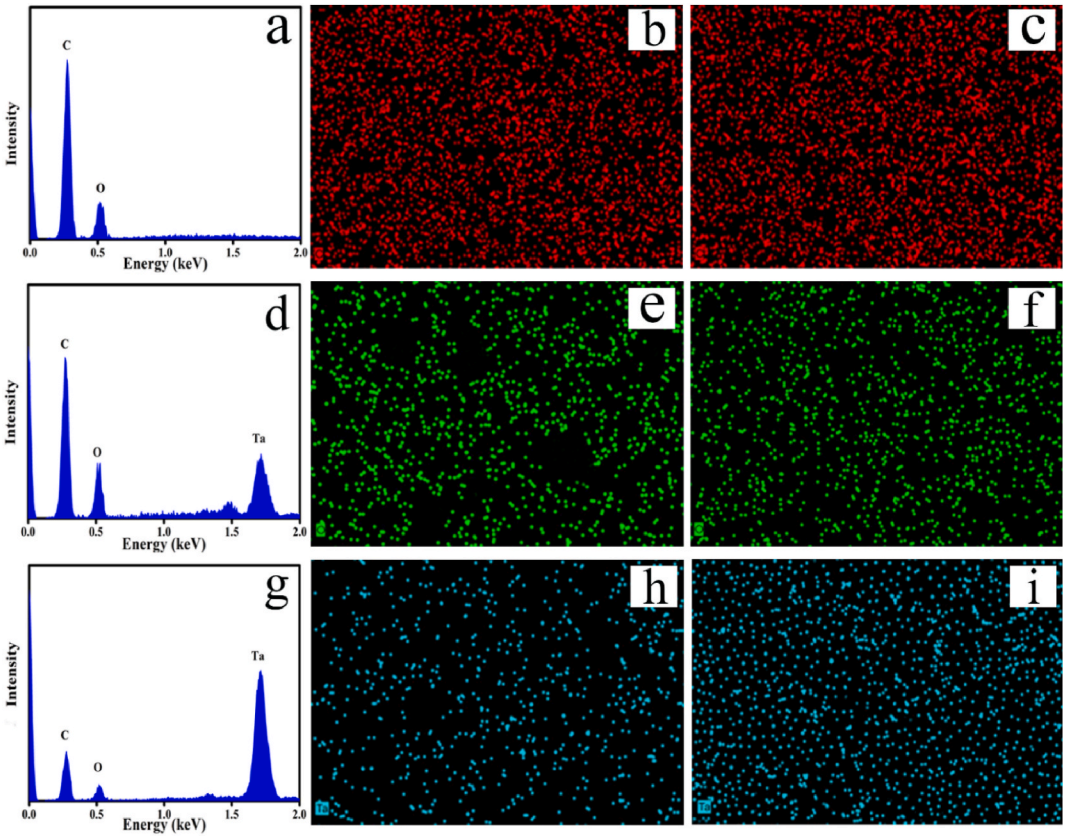

Fig. 3. EDS spectrums of PI (a), DTPC6 (d), and DTPC12 (g), and elemental mappings of C (red), O (blue), and Ta (green) for DTPC6 (b, e, h) and DTPC12 (c, f, i). (For interpretation of the references to colour in this figure legend, the reader is referred to the Web version of this article.)

days. By a prodigious difference from PI showing no layer of apatite deposits, the surface morphology of DTPC6 and DTPC12 changed and especially the DTPC12 surface was completely covered with the dense layer of apatite deposits. The layer of apatite deposits was more determined by (Fig. 6 d-i showed the EDS mapping images of PI, DTPC6, and DTPC12 after soaking into SBF for seven days. The Ca (green dots) and P (blue dots) elements were found on DTPC6 and DTPC12, and more green and blue dots were observed on

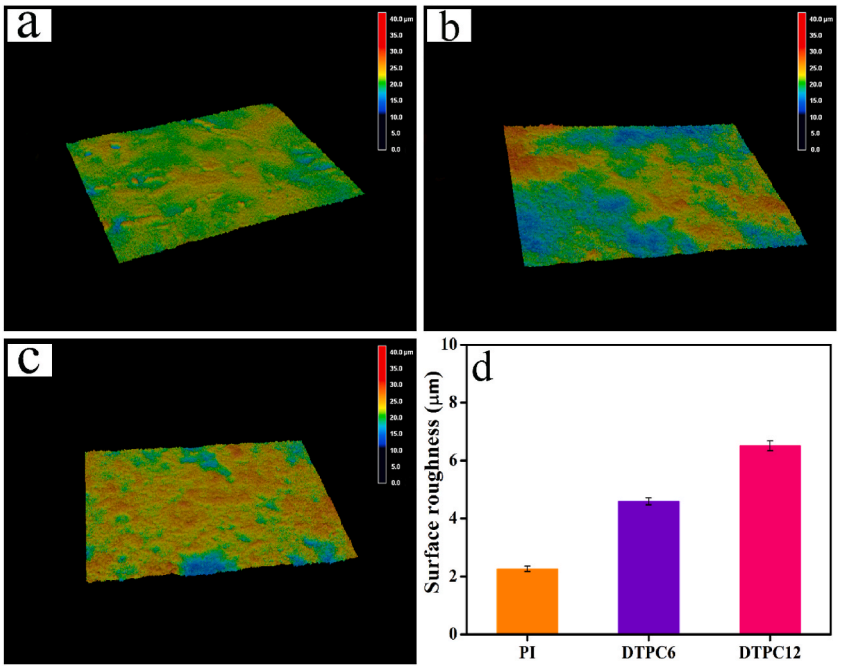

Fig. 4. Laser microscopy 3D images of PI (a), DTPC6 (b), and DTPC12 (c), and surface roughness (d).

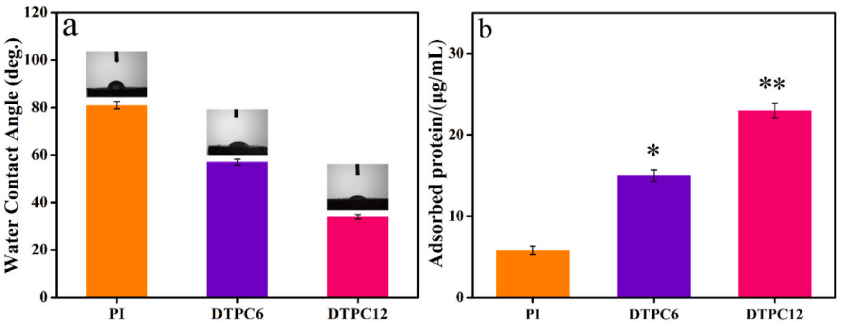

Fig. 5. Water contact angles (a) and protein adoption (b) of PI, DTPC6, and DTPC12 (*p < 0.05, vs. PI; **p < 0.01, vs. PI).

DTPC12 than on DTPC6. However, no Ca and P elements were found on the PI.) EDS detection as displayed in Fig. 6 j-l, typical spectra found from DTPC6 and DTPC12. The Ca and P peaks were observed by Ca/P ratios of 1.62 and 1.78 for DTPC6 and DTPC12, respectively, the theoretical ratio of hydroxyapatite (Ca/P = 1.67).

3.3. Cell morphology

The BMSCs morphology at 12 and 24 h on PI, DTPC6, and DTPC12 was also detected by SEM as shown in Fig. 7a–f. A small number of cells was spread and attached to the surface of PI. Consistently, the cells spread and attached well onto the DTPC6 and DTPC12 surfaces and formed a confluent layer, which showed more cells spread and attached to the DTPC12 compared with DTPC6 and PI. In particular, the DTPC12 had good biocompatibility and revealed no adverse effects on cell adhesion (see Fig. 8).

Fig. 8a-f illustrated the morphology of the rBMSC cells on PI, DTPC6, and DTPC12 stained by DAPI and FITC for 12 h. The staining of DAPI of the cells exhibited a single, semi-round cell nucleus for each cell (blue) whereas FITC staining displayed cytoplasmic for each cell (green). Good spreading morphology of cells was found on DTPC6 and DTPC12. However, just a few microfilaments of cells were observed on PI.

3.4. Cell adhesion, proliferation, and differentiation

The normalized cell attachment at 12, 24, and 48 h was displayed in Fig. 9a. It can be observed that the cell attachment on the samples improved with culture time. At 12 h, cell attachment on the DTPC6 and DTPC12 was significantly higher than PI. At 24 h and

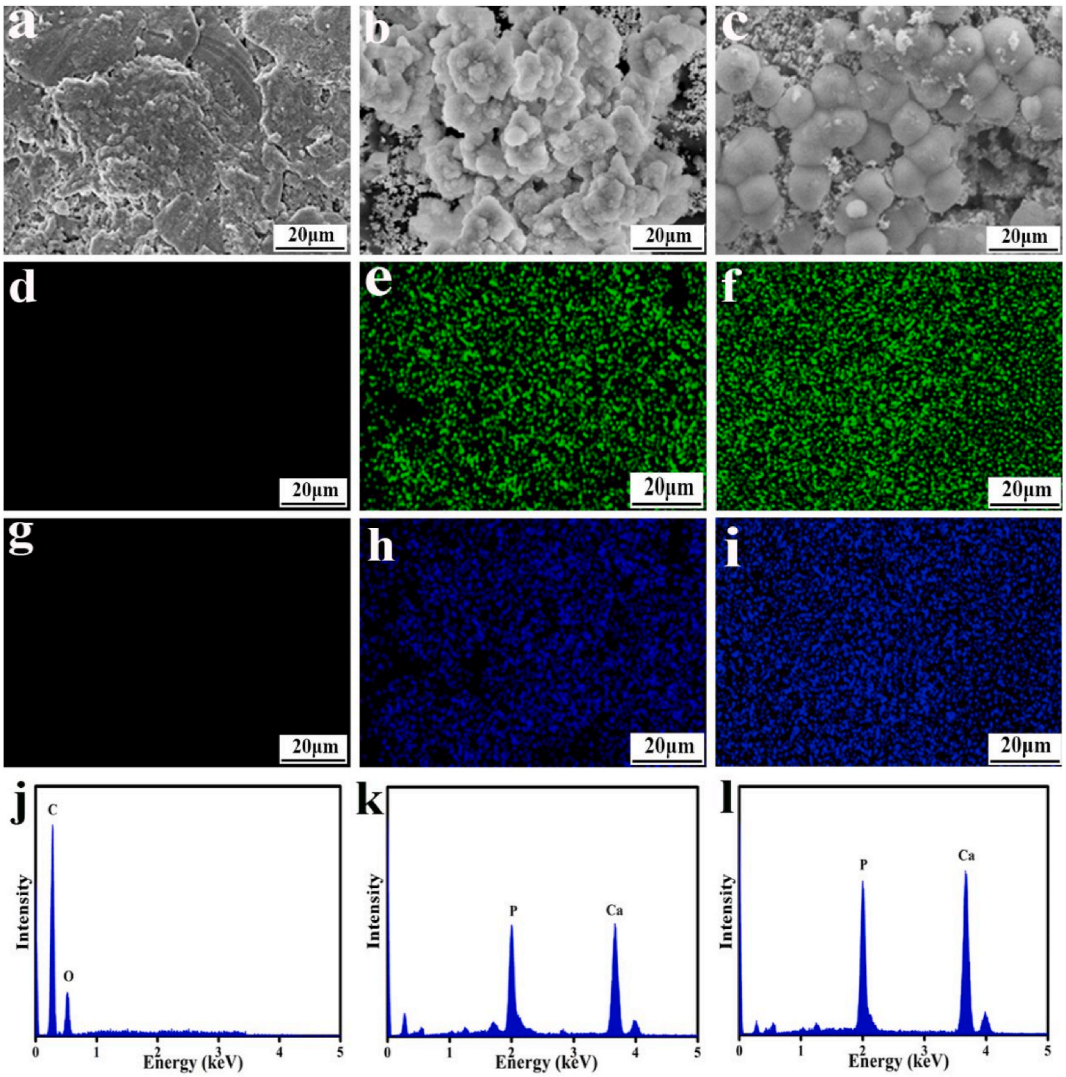

Fig. 6. SEM images of the surface morphology of PI (a), DTPC6 (b), and DTPC12 (c), EDS mapping images and EDS spectrums of PI (d, g, j), DTPC6 (e, h, k) and DTPC12 (f, i, l) after soaking into SBF for seven days (Ca: green dots; P: blue dots). (For interpretation of the references to colour in this figure legend, the reader is referred to the Web version of this article.)

48 h, a significant difference was found with increased TO content among PDA coating samples, and the difference was more evident at longer culture time (DTPC12 > DTPC6 > PI).

The BMSCs cell proliferation, characterized by the optical density (O.D.) values on PI, DTPC6, and DTPC12 was revealed in Fig. 9b and increased with culture time. However, no significant difference was found on 1 day among all the samples. The O.D. value on DTPC12 was significantly higher than DTPC6 and PI on 3 and 7 days, and DTPC12 was better than DTPC6. The results showed that in particular, DTPC12 could promote cell proliferation as compared with DTPC6 and PI.

The ALP activity is generally utilized to study the biochemical signs for the expression of osteoblast activity. The ALP activities of rBMSCs cells on PI, DTPC6, and DTPC12 are shown in Fig. 9c for 7, 10, and 14 days. The ALP activity of all samples was enhanced with culture time. At 7 days, no significant difference was observed in all samples. Moreover, the DTPC6 showed significantly higher ALP activity than DTPC6 and PI at 10 days. Furthermore, the ALP activity for DTPC12 was remarkably higher than DTPC6 and PI, with the increase of the TO content in PDA coating.

4. Discussion

Ta-based biomaterials have been extensively applied as artificial implants for orthopedic and dental applications because of their good biological properties (biocompatibility as well as bioactivity). Ta_2O_5 is the most common oxide of Ta which has favorable hydrophilicity, surface energy, and biocompatibility [37,38]. In addition, PI has been applied for biomedical applications due to its

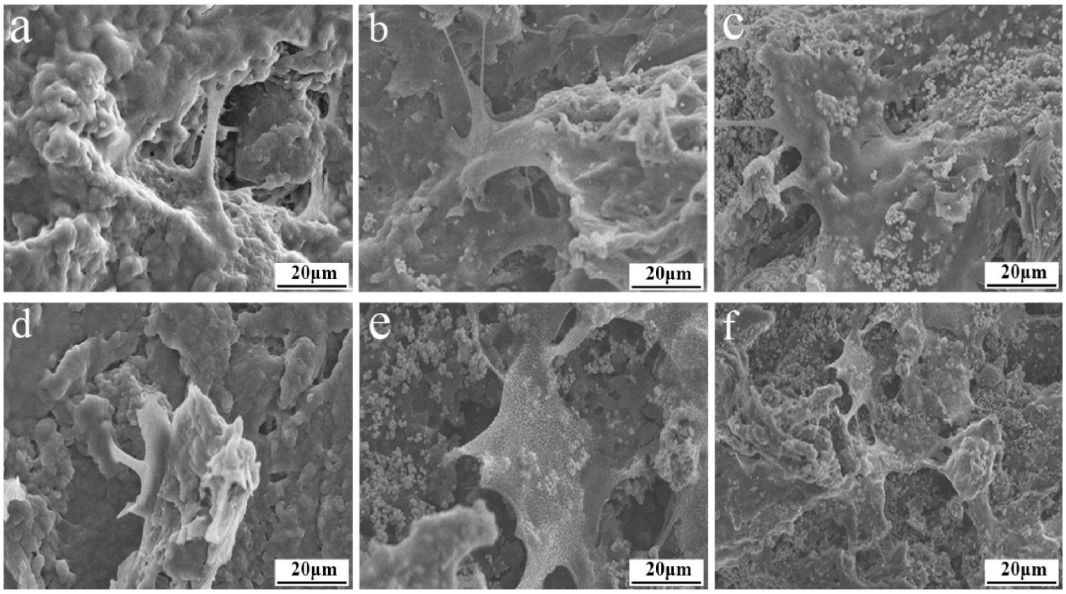

Fig. 7. SEM images of the morphology of rBMSCs on PI (a, d), DTPC6 (b, e), and DTPC12 (c, f) after cultured for 12 (a, b, c) and 24 h (d, e, f).

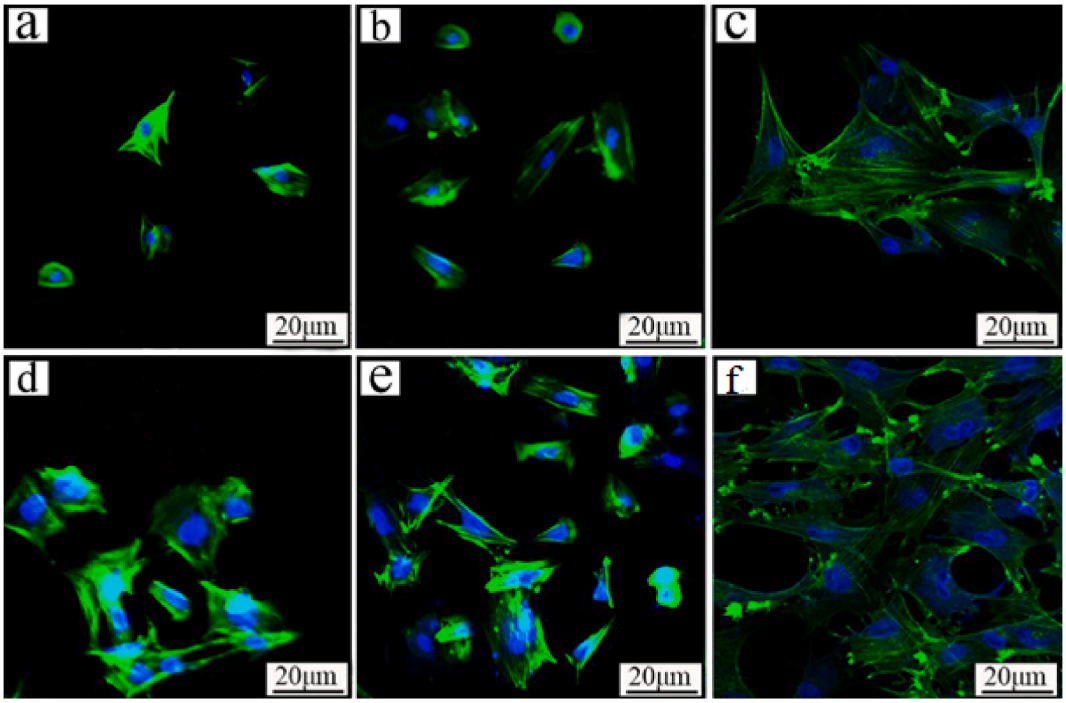

Fig. 8. CLSM photographs of the morphology of rBMSCs cultivated on PI (a, d), DTPC6 (b, e), and DTPC12 (c, f) for (a, b, c) 12 h and (d, e, f) 24 h. Nuclei in blue were stained with DAPI and the cytoskeleton in green stained with FITC. (For interpretation of the references to colour in this figure legend, the reader is referred to the Web version of this article.)

chemical resistance, and mechanical properties similar to human natural bone. However, PI has bio inertness, which limits its further applications. Moreover, surface modification for biomaterials could rapidly enhance surface bioactivity, stimulate cell responses, and ultimately improve osteointegration [39]. Herein, to enhance the bio-performances of PI, Ta_2O_5 coating was developed on the surface of PI with the bonding of PDA. The results demonstrated that the Ta_2O_5 coating was dense, and tightly bonded with the PI substrate, which dramatically improved the surface properties and bio-performances of PI.

External features such as surface morphology, hydrophilicity, roughness, and chemical composition are important in affecting cell

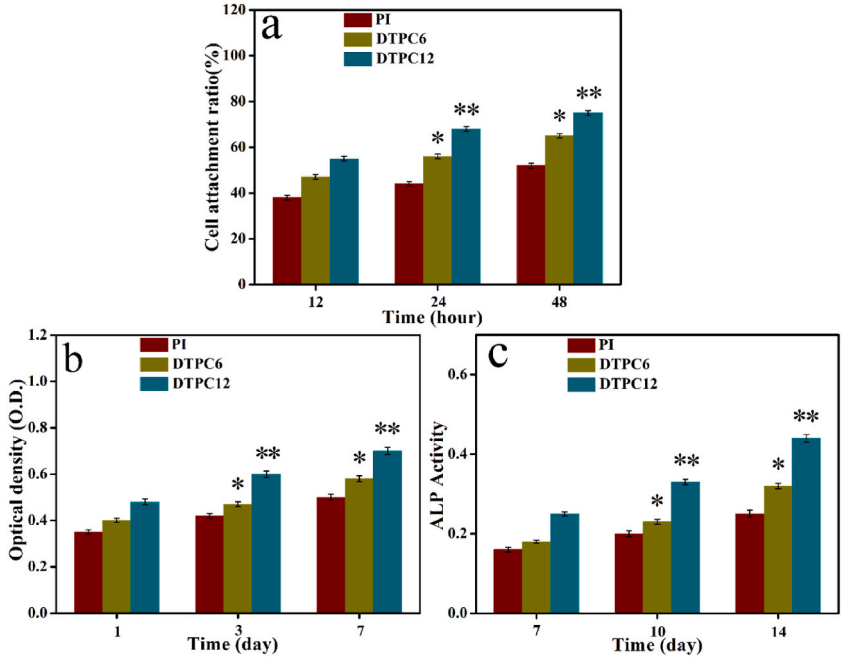

Fig. 9. Attachment ratio of rBMSCs on PI, DTPC6, and DTPC12 at 12, 24, and 48 h (a), Optical density (b), and ALP activity (c) of rBMSCs on SPI, TPSC10, and TPSC15 at different time after culturing (*p < 0.05, vs. PI; **p < 0.01, vs. PI.

responses and also have significant effects in simulating bone tissue regeneration for biomaterials [37]. The SEM images showed that Ta_2O_5 particles were bonded on the PI substrate with the bonding of PDA, and more Ta_2O_5 particles were exposed on the surface of DTPC12 than DTPC6. Moreover, compared with PI, the surface roughness of both DTPC6 and DTPC12 enhanced due to the presence of Ta_2O_5 coating, and the surface roughness of DTPC12 was higher than that of DTPC6 (PI < DTPC6 < DTPC12). The results were matched with previous studies that the Ta_2O_5 coating could improve surface roughness [40]. In addition, it was indicated that Ta_2O_5 coating improved the hydrophilicity of both DTPC6 and DTPC12 compared with PI, and DTPC12 with more Ta_2O_5 particles exhibited higher hydrophilicity than DTPC6 (PI < DTPC6 < DTPC12). It could be explained that Ta_2O_5 can spontaneously form Ta–OH groups, which can form hydrogen bonds with H_2O, indicating the improved hydrophilicity of the PI surface.

The presence of proteins adhering to the surface of biomaterials plays a crucial role in influencing cell responses, potentially leading to improved cell attachment when interacting with the biomaterial. In our study, we observed a significantly higher level of protein adsorption for DTPC12 compared to DTPC6 and PI. It has been noted that biomaterial surfaces with micro-submicron structures and hydrophilic properties tend to offer more binding sites for proteins, resulting in increased protein adsorption. Consequently, the rough and hydrophilic surface of DTPC12, attributed to its high Ta2O5 content, is likely to have a significant impact on enhancing protein adsorption [41].

The ability of apatite development and the quantity of forming apatite on the implant surface are very important for the formation of the bone tissue-material interface and can be assessed in the SBF in vitro [42,43]. In this study, there was no apatite deposition on SPI, while a considerable quantity of apatite deposition was found on the surface of both DTPC6 and DTPC12 samples, indicating that sulfonation could be useful for inducing the formation of apatite. The method of apatite formation on both DTPC6 and DTPC12 samples was related, which might be described as the induced heterogeneous nucleation of the Ta_2O_5 and polydopamine (Ta–OH) in SBF [44]. Therefore, from the results, it was confirmed that these functional groups could be helpful in fabricating apatite formation on the surface of PI.

Early cell adhesion and spreading are key factors to evaluate whether the surface of biomaterials might induce further cell behaviors [45]. Particularly, cell adhesion and proliferation are significantly essential before the osteogenic differentiation of BMSC [46]. In the current studies, the adhesion and spreading of BMSC on DTPC6 and DTPC12 were increased by the coating of Ta_2O_5, showing that Ta plays a prime role in stimulating the adhesion and spreading of BMSC, while a big amount of BMSC spread on the surface of DTPC12 compared with DTPC6 and PI.

Cell proliferation is critical to show the biocompatibility of a biomaterial and has a significant influence on the fabrication of new bone tissue in vivo. These results specified that the Ta_2O_5 coating facilitated cell attachment and spreading [47]. It was observed that the roughness and hydrophilicity of the surface might have stimulated the cell attachment and spreading. The proliferation of BMSC on DTPC6 and DTPC12 was improved by the higher Ta_2O_5 content, displaying that DTPC12 with more Ta_2O_5 content outstandingly enhanced the cell proliferation compared with both DTPC6 and PI.

Osteogenic differentiation of cells to the bio-interfaces, to the extent that bone repair biomaterials are concerned, plays an important role in the formation of bone, and ALP activity is a basic sign of cell differentiation at an initial phase of bone regeneration

[48]. Herein, the results showed that DTPC6 and DTPC12 exhibited higher ALP activity than PI, indicating that DTPC6 and DTPC12 with Ta_2O_5 coating promoted the differentiation of BMSC. Furthermore, the DTPC12 demonstrated higher ALP activity than DTPC6 and PI, indicating that the more content of Ta2O5 coating on DTPC12 had a higher effect on the differentiation of BMSC. Consequently, the improvement of the BMSC differentiation for DTPC12 was ascribed to the existence of a higher content of Ta_2O_5 coating on its surface, which could enhance its bio-performances. Consequently, it could be recommended that BMSC with improved osteogenic differentiation activity might promote new bone regeneration in vivo [49].

The cellular behaviors for example proliferation, adhesion, and differentiation of cells are remarkably affected by the different morphological properties of biomaterials (e.g. morphology, chemical composition, roughness, hydrophilicity, etc.) [50]. In the present study, the cellular behaviors for example cell proliferation, adhesion, and differentiation of DTPC6 and DTPC12 were enhanced with the coating of TO, demonstrating that the enhancements of cellular behaviors were attributed to the biological characteristics of TO coating on the surfaces with good biocompatibility, biostability and high hydrophilicity [51]. Furthermore, adhesion, proliferation, and differentiation of the cell for DTPC12 were besides enhanced compared by DTPC6 and PI, showing that the developments of the cellular behaviors to DTPC12 were ascribed to its enhanced roughness.

In a nutshell, Ta_2O_5 coating with the bonding of PDA on the PI surface enhanced the surface roughness, hydrophilicity, and protein adsorption, which could remarkably possess the optimal effects on the responses of BMSC, and DTPC12 with favorable surface properties and outstanding cytocompatibility might be applied as a great candidate for orthopedic and dental applications in coming days.

PI biocomposites coated with TO while offering several advantages for biomaterials, also present certain limitations that need to be considered. Firstly, biocompatibility remains a concern. Although TO is generally considered biocompatible, the presence of the PI surface can introduce variables that may affect the overall biocompatibility of the composite. This could lead to unforeseen immune responses or tissue reactions, making thorough biocompatibility testing imperative. Secondly, the mechanical properties of TO coated PI may not align perfectly with the needs of all biomaterial applications. PI tends to be stiff and less flexible, which can be problematic when the implant or device needs to adapt to the body's natural movements or when it must provide mechanical support. Balancing the desired properties of both materials in the composite while maintaining adequate strength and flexibility can be a significant challenge. Therefore, researchers and manufacturers should be aware of these limitations and carefully assess the suitability of TO coated PI for specific biomaterial applications, considering both biocompatibility and mechanical performance.

5. Conclusion

In this study, the modification of PI surface and coatings TO integration was performed by employing PDA suspension with TO particles. For both DTPC6 and DTPC12, the surface roughness, hydrophilicity, apatite mineralization, and coatings including TO particles were significantly greater than PI. In comparison to DTPC6 and PI, DTPC12 with high TO content demonstrated improved surface properties. In addition, the adhesion and proliferation response of BMSC remarkably improved as compared to those of DTPC6 and DTPC12, while the best cellular response was induced by DTPC12. In short, the TO particles coating of DTPC12 including high TO content has an appreciable potential to act as a biomaterial for dental and orthopedic applications because of considerable improvements in their surface properties, bioactivity, and cytocompatibility. Cell culture results showed that PI surface coating Ta_2O_5 could enhance the proliferation, adhesion, and osteogenic differentiation of BMSCs. The outcomes confirmed that fabricating Ta_2O_5 coating on the surface of PI by PDA bonding could improve the biocompatibility in addition to the bioactivity of PI, and increase the application potential of PI in the field of bone repair materials.

Informed consent statement

This study was not performed on humans.

Funding

The authors received no specific funding for this work.

Data availability statement

No data was used for the research described in the article.

CRediT authorship contribution statement

Syed Asadullah: Methodology, Formal analysis, Conceptualization. **Mahmood Ahmed:** Writing – review & editing, Writing – original draft, Formal analysis. **Sadaf Sarfraz:** Resources, Formal analysis. **Manzar Zahra:** Visualization, Data curation. **Asnuzilawati Asari:** Formal analysis. **Nurul Huda Abdul Wahab:** Validation. **Farah Sobia:** Writing – review & editing. **Dure Najaf Iqbal:** Formal analysis.

Declaration of competing interest

The authors declare that they have no known competing financial interests or personal relationships that could have appeared to influence the work reported in this paper.

References

[1] W. Wang, K.W. Yeung, Bone grafts and biomaterials substitutes for bone defect repair: a review, Bioact. Mater. 2 (4) (2017) 224–247.
[2] J. Du, et al., Surface polydopamine modification of bone defect repair materials: characteristics and applications, Front. Bioeng. Biotechnol. 10 (2022), 974533.
[3] M. Kaur, K. Singh, Review on titanium and titanium based alloys as biomaterials for orthopaedic applications, Mater. Sci. Eng. C 102 (2019) 844–862.
[4] R.S. Mishra, et al., Mechanical behavior and superplasticity of a severe plastic deformation processed nanocrystalline Ti–6Al–4V alloy, Mater. Sci. Eng. 298 (1–2) (2001) 44–50.
[5] Q. Yi, et al., Improvement of polydopamine-loaded salidroside on osseointegration of titanium implants, Chin. Med. 17 (1) (2022) 26.
[6] L. Wang, et al., Polyetheretherketone/nano-fluorohydroxyapatite composite with antimicrobial activity and osseointegration properties, Biomaterials 35 (25) (2014) 6758–6775.
[7] L. Shi, et al., The improved biological performance of a novel low elastic modulus implant, PLoS One 8 (2) (2013), e55015.
[8] W.C. Head, D.J. Bauk, R.H. Emerson Jr., Titanium as the material of choice for cementless femoral components in total hip arthroplasty, Clin. Orthop. Relat. Res. 311 (1995) 85–90, 1976-2007.
[9] B.V. Krishna, S. Bose, A. Bandyopadhyay, Low stiffness porous Ti structures for load-bearing implants, Acta Biomater. 3 (6) (2007) 997–1006.
[10] Y. Zhou, et al., Polydopamine-coated biomimetic bone scaffolds loaded with exosomes promote osteogenic differentiation of BMSC and bone regeneration, Regenerative Therapy 23 (2023) 25–36.
[11] J.-Y. Lee, et al., Enhanced bone formation by controlled growth factor delivery from chitosan-based biomaterials, J. Contr. Release 78 (1–3) (2002) 187–197.
[12] J.-Y. Lee, et al., Transforming growth factor (TGF)-β1 releasing tricalcium phosphate/chitosan microgranules as bone substitutes, Pharmaceut. Res. 21 (2004) 1790–1796.
[13] C. Peng, et al., Surface modification of silk fibroin composite bone scaffold with polydopamine coating to enhance mineralization ability and biological activity for bone tissue engineering, J. Appl. Polym. Sci. 139 (38) (2022), e52900.
[14] H.-W. Kim, J.C. Knowles, H.-E. Kim, Hydroxyapatite porous scaffold engineered with biological polymer hybrid coating for antibiotic Vancomycin release, J. Mater. Sci. Mater. Med. 16 (2005) 189–195.
[15] C. Soundrapandian, B. Sa, S. Datta, Organic–inorganic composites for bone drug delivery, AAPS PharmSciTech 10 (2009) 1158–1171.
[16] S. Asadullah, et al., Preparation, characterization, in vitro bioactivity and rBMSCs responses to tantalum pentoxide/polyimide biocomposites for dental and orthopedic implants, Compos. B Eng. 177 (2019), 107433.
[17] Z. Fekete, A. Pongrácz, Multifunctional soft implants to monitor and control neural activity in the central and peripheral nervous system: a review, Sensor. Actuator. B Chem. 243 (2017) 1214–1223.
[18] X. Navarro, et al., A critical review of interfaces with the peripheral nervous system for the control of neuroprostheses and hybrid bionic systems, J. Peripher. Nerv. Syst. 10 (3) (2005) 229–258.
[19] L. Kong, et al., Polydopamine coating with static magnetic field promotes the osteogenic differentiation of human bone-derived mesenchymal stem cells on three-dimensional printed porous titanium scaffolds by upregulation of the BMP-Smads signaling pathway, American Journal of Translational Research 12 (12) (2020) 7812.
[20] A. Soltani, Application of cavitation promoting surfaces in management of acute ischemic stroke, Ultrasonics 53 (2) (2013) 580–587.
[21] A. Koutroulis, et al., Investigation of the effect of the water to powder ratio on hydraulic cement properties, Dent. Mater. 35 (8) (2019) 1146–1154.
[22] H. Tolabi, et al., A critical review on polydopamine surface-modified scaffolds in musculoskeletal regeneration, Front. Bioeng. Biotechnol. 10 (2022), 1008360.
[23] Q. Cheng, et al., Regulation of surface micro/nano structure and composition of polyetheretherketone and their influence on the behavior of MC3T3-E1 pre-osteoblasts, J. Mater. Chem. B 7 (37) (2019) 5713–5724.
[24] B. Yuan, et al., Comparison of osteointegration property between PEKK and PEEK: effects of surface structure and chemistry, Biomaterials 170 (2018) 116–126.
[25] L. Ouyang, et al., Influence of sulfur content on bone formation and antibacterial ability of sulfonated PEEK, Biomaterials 83 (2016) 115–126.
[26] J.-l. Wang, et al., Electropolymerization of dopamine for surface modification of complex-shaped cardiovascular stents, Biomaterials 35 (27) (2014) 7679–7689.
[27] T.-Y. Kuo, et al., Mechanical and biological properties of graded porous tantalum coatings deposited on titanium alloy implants by vacuum plasma spraying, Surf. Coating. Technol. 372 (2019) 399–409.
[28] L. Li, et al., Polydopamine coating promotes early osteogenesis in 3D printing porous Ti6Al4V scaffolds, Ann. Transl. Med. 7 (11) (2019).
[29] S. Kim, et al., Antibacterial and bioactive properties of stabilized silver on titanium with a nanostructured surface for dental applications, Appl. Surf. Sci. 451 (2018) 232–240.
[30] L. Wang, et al., Surface hydroxylation regulates cellular osteogeneses on TiO2 and Ta2O5 nanorod films, Colloids Surf. B Biointerfaces 167 (2018) 213–219.
[31] B.-S. Moon, et al., Hierarchical micro-nano structured Ti6Al4V surface topography via two-step etching process for enhanced hydrophilicity and osteoblastic responses, Mater. Sci. Eng. C 73 (2017) 90–98.
[32] M. Yu, et al., Surface hydroxyl groups regulate the osteogenic differentiation of mesenchymal stem cells on titanium and tantalum metals, J. Mater. Chem. B 5 (21) (2017) 3955–3963.
[33] M. Tanomaru-Filho, et al., Biocompatibility and mineralized nodule formation of Neo MTA Plus and an experimental tricalcium silicate cement containing tantalum oxide, Int. Endod. J. 50 (2017) e31–e39.
[34] N. Horandghadim, J. Khalil-Allafi, M. Urgen, Effect of Ta2O5 content on the osseointegration and cytotoxicity behaviors in hydroxyapatite-Ta2O5 coatings applied by EPD on superelastic NiTi alloys, Mater. Sci. Eng. C 102 (2019) 683–695.
[35] N. Rocton, et al., Fine analysis of interaction mechanism of bioactive glass surface after soaking in SBF solution: AFM and ICP-OES investigations, Appl. Surf. Sci. 505 (2020), 144076.
[36] F. Baino, S. Yamaguchi, The use of simulated body fluid (SBF) for assessing materials bioactivity in the context of tissue engineering: review and challenges, Biomimetics 5 (4) (2020) 57.
[37] B. Rahmati, et al., Development of tantalum oxide (Ta-O) thin film coating on biomedical Ti-6Al-4V alloy to enhance mechanical properties and biocompatibility, Ceram. Int. 42 (1) (2016) 466–480.
[38] M. Li, et al., Dopamine modified organic–inorganic hybrid coating for antimicrobial and osteogenesis, ACS Appl. Mater. Interfaces 8 (49) (2016) 33972–33981.
[39] P. Zhou, et al., Rapidly-deposited polydopamine coating via high temperature and vigorous stirring: formation, characterization and biofunctional evaluation, PLoS One 9 (11) (2014), e113087.
[40] L. Bai, et al., Differential effect of hydroxyapatite nano-particle versus nano-rod decorated titanium micro-surface on osseointegration, Acta Biomater. 76 (2018) 344–358.
[41] S. Asadullah, et al., Sulfonated porous surface of tantalum pentoxide/polyimide composite with micro-submicro structures displaying antibacterial performances and stimulating cell responses, Mater. Des. 190 (2020), 108510.
[42] Y. Zhao, et al., Cytocompatibility, osseointegration, and bioactivity of three-dimensional porous and nanostructured network on polyetheretherketone, Biomaterials 34 (37) (2013) 9264–9277.
[43] F. Zhao, et al., The effects of surface properties of nanostructured bone repair materials on their performances, J. Nanomater. 2015 (2015), 10-10.

[44] A. Jaggessar, et al., Bio-mimicking nano and micro-structured surface fabrication for antibacterial properties in medical implants, J. Nanobiotechnol. 15 (2017) 1–20.
[45] B.D. Boyan, E.M. Lotz, Z. Schwartz, Roughness and hydrophilicity as osteogenic biomimetic surface properties, Tissue Eng. 23 (23–24) (2017) 1479–1489.
[46] M. Hoyos-Nogués, et al., All-in-one trifunctional strategy: a cell adhesive, bacteriostatic and bactericidal coating for titanium implants, Colloids Surf. B Biointerfaces 169 (2018) 30–40.
[47] A. Ahmad Khalili, M.R. Ahmad, A review of cell adhesion studies for biomedical and biological applications, Int. J. Mol. Sci. 16 (8) (2015) 18149–18184.
[48] Q. Tang, et al., Microporous polysaccharide multilayer coated BCP composite scaffolds with immobilised calcitriol promote osteoporotic bone regeneration both in vitro and in vivo, Theranostics 9 (4) (2019) 1125.
[49] B.-Q. Chen, et al., Investigation of silk fibroin nanoparticle-decorated poly (l-lactic acid) composite scaffolds for osteoblast growth and differentiation, Int. J. Nanomed. 12 (2017) 1877.
[50] Y. Qin, et al., Bone marrow stromal/stem cell-derived extracellular vesicles regulate osteoblast activity and differentiation in vitro and promote bone regeneration in vivo, Sci. Rep. 6 (1) (2016), 21961.
[51] W. Wang, et al., The in vitro and in vivo biological effects and osteogenic activity of novel biodegradable porous Mg alloy scaffolds, Mater. Des. 189 (2020), 108514.